nature neuroscience

PI3K promotes voltage-dependent calcium channel trafficking to the plasma membrane

Patricia Viard[1], Adrian J Butcher[1,4], Guillaume Halet[2,4], Anthony Davies[1], Bernd Nürnberg[3], Fay Heblich[1] & Annette C Dolphin[1]

Phosphatidylinositol 3-kinase (PI3K) has been shown to enhance native voltage-dependent calcium channel (Ca_v) currents both in myocytes and in neurons; however, the mechanism(s) responsible for this regulation were not known. Here we show that PI3K promotes the translocation of GFP-tagged Ca_v channels to the plasma membrane in both COS-7 cells and neurons. We show that the effect of PI3K is mediated by Akt/PKB and specifically requires $Ca_v\beta_2$ subunits. The mutations S574A and S574E in $Ca_v\beta_{2a}$ prevented and mimicked, respectively, the effect of PI3K/Akt-PKB, indicating that phosphorylation of Ser574 on $Ca_v\beta_{2a}$ is necessary and sufficient to promote Ca_v channel trafficking.

Ca_v channels are an important route for the entry of Ca^{2+} into excitable cells, where it is required for numerous physiological events[1,2]. Ca_v channels are opened upon membrane depolarization; however, the amplitude of Ca^{2+} influx is also controlled by extracellular signals binding to membrane receptors and relayed by transduction effectors including G-proteins and phosphatidylinositol 3-kinases (PI3Ks). In vascular myocytes, PI3K mediates the increase of L-type current produced by Gβγ dimers released upon stimulation by angiotensin II mediated by the G-protein-coupled receptor (GPCR) $AT1_A$[3]. In cerebellar granule neurons, the stimulation of both native L- and N-type Ca_v channels induced by insulin-like growth factor (IGF-1), which binds to tyrosine kinase–associated receptors (TKRs), is also mediated by PI3K[4].

PI3Ks are lipid kinases that phosphorylate phosphoinositides on position 3 of their inositol head group. The two main phosphoinositide products created in response to extracellular stimuli are $PI(3,4)P_2$ and $PI(3,4,5)P_3$, also called PIP_3 (ref. 5). Both bind to pleckstrin homology domains of their effectors, such as phosphoinositide-dependent kinase (PDK1) and protein kinase B (PKB, also called Akt), inducing their translocation from the cytosol to the plasma membrane[5,6]. There are several isoforms of PI3Ks, classified according to their *in vitro* lipid substrate specificity and their activation pathway[5,7]. Although activation, respectively, of PI3Kγ by the TKR-activated small G-protein ras[8,9] and of PI3Kβ by GPCRs[10] has also been reported, TKRs are generally associated with the activation of PI3Kα, -β and -δ and GPCRs with the activation of PI3Kγ. Indeed, in vascular myocytes, infusion of PI3Kγ reproduces the Gβγ-mediated effect of angiotensin II[3], whereas in neurons, overexpression of PI3Kα mimics the effect of the TKR agonist IGF-1 (ref. 4).

Thus it is clear that several activation pathways and several isoforms of PI3K can modulate Ca^{2+} entry. However, both the signal transduction pathway activated downstream of PI3K and the underlying mechanism(s) leading to the increased Ca^{2+} influx remain to be elucidated.

High-voltage-activated Ca_v channels are composed *in vivo* of $Ca_v\alpha1$, β, $\alpha_2\delta$ and potentially γ subunits[1,2]. To investigate whether the composition of the Ca_v channels is a determinant for their sensitivity to PI3K, as well as to identify the elements required for such regulation, we expressed both PI3Ks and cloned Ca_v channels in COS-7 cells. We demonstrate, first, that PI3K increases the expression of functional Ca_v channels at the plasma membrane and, second, that this regulation occurs for channels associated with a specific $Ca_v\beta$ subunit: $Ca_v\beta_2$. The PI3K-induced regulation is mediated by PIP_3-activated Akt/PKB and requires the phosphorylation of $Ca_v\beta_2$ subunits on a unique serine residue. Both PI3Kγ and PI3Kα increased the expression of Ca_v channels at the plasma membrane, indicating that this regulation is not specific to one PI3K isoform. In neurons, we show that acute stimulation of PI3K by TKR also induces the translocation of GFP-tagged Ca_v channels to the plasma membrane. Thus, our results indicate that PI3K-induced regulation of Ca_v channel trafficking may be a general mechanism for the regulation of calcium entry in excitable cells.

RESULTS

PI3K-induced regulation of Ca_v currents

We cotransfected COS-7 cells with both the catalytic subunit p110γ and the associated protein p101 to express PI3Kγ. The expression of both proteins was confirmed by western blotting (**Fig. 1a**). No expression of p110γ was detected in control cells, indicating that PI3Kγ was not endogenously expressed in COS-7 cells, as has previously been reported[11].

PI3Kγ has been shown to have significant basal activity in the absence of Gβγ *in vitro*[12]. In COS-7 cells, the endogenous pool of free

[1]Department of Pharmacology and [2]Department of Physiology, University College London, London WC1E 6BT, UK. [3]Institut für Biochemie und Molekular Biologie II, Klinikum der Heinrich-Heine-Universität Düsseldorf, 40225 Düsseldorf, Germany. [4]These authors contributed equally to this work. Correspondence should be addressed to P.V. (p.viard@ucl.ac.uk).

Published online 15 August 2004; doi:10.1038/nn1300

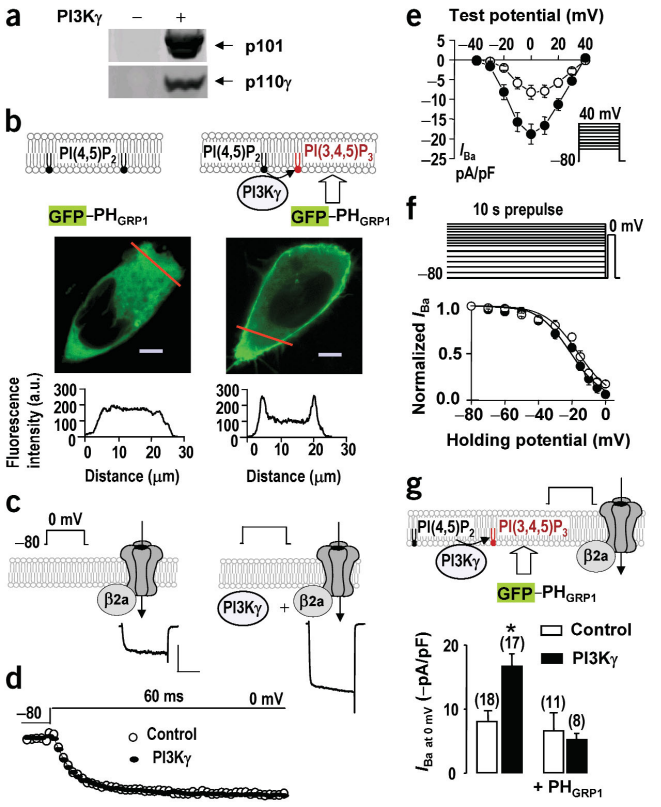

Figure 1 Effect of PI3Kγ-induced production of PIP3 on $Ca_v1.2\alpha1/\beta_{2a}$ currents. (**a**) Immunodetection of PI3Kγ in control and PI3Kγ-transfected cells. p101 (upper row, arrow) was detected in PI3Kγ-transfected cells using an antibody to its EE-tag. The p110γ antibody revealed expression of p110γ (lower row, arrow) in PI3Kγ-transfected cells only. (**b**) Subcellular localization of PH_{Grp1}-GFP in control (left) and PI3Kγ-transfected cells (right) with line scans below the image taken at the position indicated by the red bar. a.u., arbitrary units. Scale bars (in white), 10 μm. (**c**) Sample current traces of $Ca_v1.2\alpha1/\beta_{2a}$ I_{Ba} recorded in control and PI3Kγ-transfected cells. Vertical and horizontal calibration bars are 10 pA/pF and 100 ms, respectively. (**d**) Averaged and normalized I_{Ba} traces recorded from cells expressing $Ca_v1.2\alpha1/\beta_{2a}$ channels without (Control) and with PI3Kγ ($n = 20$). (**e**,**f**) Mean *I-V* (**e**) and steady-state inactivation relationship (**f**) of $Ca_v1.2\alpha1/\beta_{2a}$ I_{Ba} in control (○) and PI3Kγ-transfected cells (●). The voltage protocols are indicated. Current densities are shown as mean ± s.e.m. of 22–26 cells (**e**) and 5–9 cells (**f**). (**g**) Effect of overexpressed PH_{Grp1}-GFP on $Ca_v1.2\alpha1/\beta_{2a}$ I_{Ba} control cells or PI3Kγ- and $Ca_v1.2\alpha1/\beta_{2a}$ transfected cells. The number of experiments is given in parentheses. $^*P < 0.05$ as compared to control.

Gβγ[13] may stimulate the activity of transfected PI3Kγ, and PI3Kγ expressed without further activation in these cells can increase the total content of PIP_3 (ref. 14). To determine whether the heterologously expressed PI3Kγ was functional and active, we cotransfected the cells with the GFP-tagged pleckstrin homology domain of the general receptor for phosphoinositides (PH_{Grp1}-GFP), which specifically binds PIP_3[15]. Intensity profiles highlight the increase in fluorescence occurring at the plasma membrane. PH_{Grp1}-GFP domains were homogeneously distributed in control cells (**Fig. 1b**, left). In contrast, in PI3Kγ-transfected cells, PH_{Grp1}-GFP was largely recruited to the cell membrane, indicating that PIP_3 was elevated (**Fig. 1b**, right). The relative increase in PH_{Grp1}-GFP plasma membrane localization as compared to cytosol in PI3Kγ-transfected cells was 56 ± 4% ($n = 10$ cells). The nucleus, visualized through a decrease in fluorescence (**Fig. 1b**) or stained with Hoechst 33342 (**Supplementary Fig. 1** online), is not responsible for the accumulation of green fluorescence observed at the periphery of the PI3Kγ-transfected cells.

We then assessed the effect of PI3Kγ on Ca_v channels. PI3Kγ expression resulted in higher calcium channel current densities (I_{Ba}) in cells expressing $Ca_v1.2\alpha1/\beta_{2a}$ (by 130 ± 31%; $n = 22$ at 0 mV) (**Fig. 1c**). We also assessed the effect of PI3K in the presence of α2δ subunits (data not shown): we observed a similar increase, of 151 ± 44%, in the presence of α2δ-1 ($n = 3$; $P < 0.05$). This is consistent with the effects reported to occur after physiological stimulation of native L- and N-type currents[3,4]. The maximum conductance was twice as high in PI3Kγ-transfected cells as in controls: 0.60 ± 0.09 nS/pF as compared to 0.30 ± 0.05 nS/pF ($n = 26$; $P < 0.005$). No differences in the kinetics of activation or inactivation of the average normalized current traces were detected between control and PI3Kγ-transfected cells (**Fig. 1d**), although the effect of PI3Kγ resulted in a small hyperpolarization of the current density–voltage (*I-V*) relationship (by –5.2 ± 1.2 mV; $P < 0.005$) (**Fig. 1e**). The voltage dependence of steady-state inactivation remained unchanged (**Fig. 1f**).

PI3Kγ has a dual role of protein and lipid kinase. The protein kinase activity is required for the activation of the mitogen-activated protein kinase, whereas phosphorylated PIs recruit and activate other kinases, such as Akt/PKB[16]. To assess the involvement of PIP_3 in the PI3Kγ-

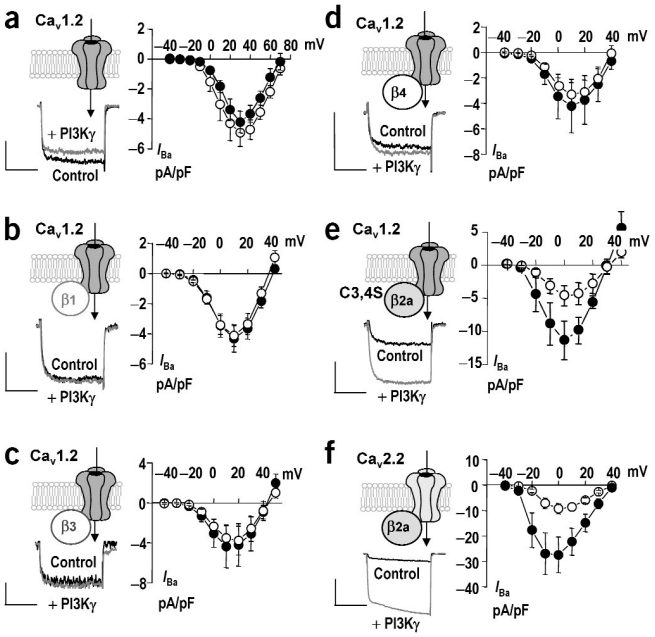

Figure 2 Relevance of Ca_v subunit composition for PI3Kγ effect on I_{Ba}. (**a**–**f**) Sample current traces and mean *I-V* relationship of channels formed by (**a**) $Ca_v1.2\alpha1$ alone (**b**) $Ca_v1.2\alpha1/\beta_{1b}$ (**c**) $Ca_v1.2\alpha1/\beta_3$ (**d**) $Ca_v1.2\alpha1/\beta_4$ (**e**) $Ca_v1.2\alpha1/\beta_{2a(C3,4S)}$ and (**f**) $Ca_v2.2\alpha1/\beta_{2a}$ channels in control (○) and PI3Kγ-transfected cells (●). The illustrated current traces were elicited by a depolarization from –80 to +20 mV (**a**), 0 mV (**b**–**e**) and –10 mV (**f**). Vertical calibration bars are 3 pA/pF in **a**–**d**, 5 pA/pF in **e** and 20 pA/pF in **f**. In the absence of $Ca_v\beta$ subunits (**a**), the concentration of charge carrier was increased from 1 to 10 mM to allow measurement of current densities comparable to those recorded with $Ca_v\beta_{1b}$, β_3 or β_4. Horizontal calibration bars are 100 ms. Current densities are shown as mean ± s.e.m. of 6–22 COS-7 cells.

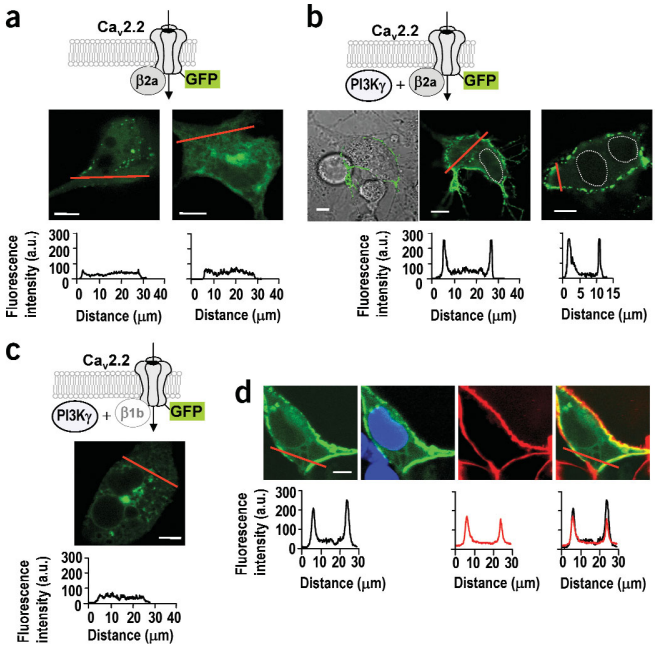

Figure 3 Effect of PI3Kγ on Ca_v channel membrane localization. (**a**,**b**) Subcellular localization of GFP-$Ca_v2.2\alpha1/\beta_{2a}$ in control (**a**) or in PI3Kγ-cotransfected cells (**b**). (**c**) Subcellular localization of GFP-$Ca_v2.2\alpha1/\beta_{1b}$ in PI3Kγ-cotransfected cells. (**d**) First panel, subcellular localization of GFP-$Ca_v2.2\alpha1/\beta_{2a}$ in a PI3Kγ-transfected cell. Second panel, overlay of the GFP-$Ca_v2.2\alpha1/\beta_{2a}$ fluorescence image and nuclear staining with Hoechst 33342. Third panel, membrane staining with FM4-64. The intensity profile of FM4-64 fluorescence is indicated in red. Fourth panel, overlay of the fluorescence images showing GFP-$Ca_v2.2\alpha1/\beta_{2a}$ and the membrane marker FM4-64. Scale bars, 10 μm.

induced enhancement of Ca_v currents, we coexpressed PI3Kγ with the PH_{Grp1}-GFP domain and the Ca_v channels. This prevented the PI3Kγ-induced increase of $Ca_v1.2\alpha1/\beta_{2a}$ I_{Ba} while not significantly affecting the control level (**Fig. 1g**), indicating that PI3Kγ upregulates Ca_v current through production of PIP_3.

Relevance of Ca_v channel subunit composition

To determine whether $Ca_v\beta$ subunits were required for the response to PI3Kγ, COS-7 cells were transfected with the pore-forming $Ca_v1.2\alpha1$ alone or in association with different $Ca_v\beta$ subunits. There was no difference in I_{Ba} between control and PI3Kγ-transfected cells in the absence of $Ca_v\beta$ subunits (**Fig. 2a**). Furthermore, cells cotransfected with either $Ca_v\beta_{1b}$, $Ca_v\beta_3$ or $Ca_v\beta_4$ did not show any modulation by PI3Kγ (**Fig. 2b–d**), indicating that the PI3Kγ-induced modulation specifically requires $Ca_v\beta_{2a}$ coexpression. One unique property of $Ca_v\beta_{2a}$ as compared to the other $Ca_v\beta$ subunits is that it is palmitoylated[17]. Coexpressing $Ca_v1.2\alpha1$ and a palmitoylation-deficient β_{2a}(C3,4S)[18] did not prevent PI3Kγ-induced enhancement of I_{Ba} and hyperpolarization of the *I-V* relationship (**Fig. 2e**), indicating that palmitoylation of $Ca_v\beta_{2a}$ is not responsible for the specificity of the effect. When coexpressed with $Ca_v2.2\alpha1$, $Ca_v\beta_{2a}$ also conferred sensitivity to PI3Kγ on N-type channels (**Fig. 2f**), indicating that PI3Kγ-induced modulation is not specific to one type of Ca_v channel. In this case, the maximum conductance was increased from 0.27 ± 0.05 nS/pF (n = 22) in controls to 0.77 ± 0.17 nS/pF (n = 17; $P < 0.005$) in PI3Kγ-transfected cells.

Effect of PI3Kγ on Ca_v membrane expression

$Ca_v\beta$ subunits have a chaperone-like role in the trafficking of $Ca_v\alpha1$ subunits to the plasma membrane[19,20]. In addition, PI3K has been reported to be involved in the membrane expression of cationic channels[21]. To investigate whether the enhancement of Ca_v maximum conductance induced by PI3Kγ could be due to an increased expression of Ca_v channels at the plasma membrane, we examined the subcellular distribution of GFP-tagged $Ca_v2.2\alpha1$, which produces functional channels with current amplitudes comparable to those of untagged $Ca_v2.2$ channels[22]. In the absence of PI3Kγ, the GFP-$Ca_v2.2\alpha1/\beta_{2a}$ channels seemed largely to be located throughout the cells either rather homogeneously (**Fig. 3a**, left) or with some intracellular retention, mostly in the perinuclear region (**Fig. 3a**, right), where they colocalized with an endoplasmic reticulum marker (ER-Tracker Blue-White DPX; data not shown). In cells transfected with PI3Kγ, GFP-positive cells showed distinct plasma membrane localization of the GFP-$Ca_v2.2\alpha1/\beta_{2a}$ channels. The GFP-$Ca_v2.2\alpha1$ staining either appeared continuous (**Fig. 3b**, left and middle) or formed punctate clusters at the plasma membrane (**Fig. 3b**, right). The relative increase in plasma membrane as compared to cytosolic localization, measured along the intensity profiles, was 83 ± 2% (n = 25 cells). This strong plasma membrane staining was visible on all focal planes of acquisition (**Supplementary Video 1** online). As predicted by the electrophysiological experiments, GFP-$Ca_v2.2$ cotransfected with $Ca_v\beta_{1b}$ subunits (**Fig. 3c**) did not accumulate at the cell surface in response to PI3Kγ overexpression, and its distribution was similar to that seen for the control, and as previously described[22]. We showed that the nucleus, visualized through a decrease in fluorescence (**Fig. 3d**, first panel) or stained with Hoechst 33342 (**Fig. 3d**, second panel), is not responsible for the accumulation of green fluorescence observed at the periphery of the PI3K-transfected cells. Furthermore, overlay of the green fluorescence either with the bright-field image (**Fig. 3b**, left) or with the red fluorescence emitted by the plasma membrane marker FM4-64 (**Fig. 3d**, third and fourth panels) clearly indicated that GFP-$Ca_v2.2\alpha1/\beta_{2a}$ channels are integrated at the plasma membrane.

Role of Akt/PKB in Ca_v channel trafficking

We next examined the pathway downstream of PI3Kγ. Akt/PKB has been reported to be involved in the translocation of membrane proteins[23]. PIP_3 binds to the pleckstrin homology domain of Akt/PKB, translocating it to the inner surface of the plasma membrane where it is phosphorylated and activated on Thr308 by the PIP_3-stimulated PDK1 and on Ser473 by another, less well understood, serine kinase[5–7]. Expression of endogenous PDK1 in COS-7 cells was confirmed by immunoblotting (data not shown). We found that Akt/PKB was phosphorylated on Thr308 (**Fig. 4a**, left) and on Ser473 (**Fig. 4a**, right) in PI3Kγ-transfected cells, indicating that heterologous expression of PI3Kγ activates endogenous Akt/PKB.

We first assessed the involvement of Akt/PKB in both the PI3Kγ-induced increase in I_{Ba} and the targeting of GFP-$Ca_v2.2$ channels by using the dominant-negative mutant AAA-Akt/PKB[24], which has been shown to prevent activation of endogenous Akt/PKB both in HEK-293 cells[24] and in myoblasts[23]. Coexpression of AAA-Akt/PKB with PI3Kγ significantly reduced accumulation of GFP-$Ca_v2.2\alpha1/\beta_{2a}$ at the plasma membrane in three independent experiments (**Fig. 4b**), leaving only 25 ± 5% of the cells showing any obvious membrane expression. This proportion was significantly lower than the 69 ± 3% of cells showing GFP-$Ca_v2.2\alpha1/\beta_{2a}$ accumulation at the membrane in cultures transfected in parallel with PI3Kγ without AAA-Akt/PKB. Cotransfection of the AAA-Akt/PKB mutant with PI3Kγ also pre-

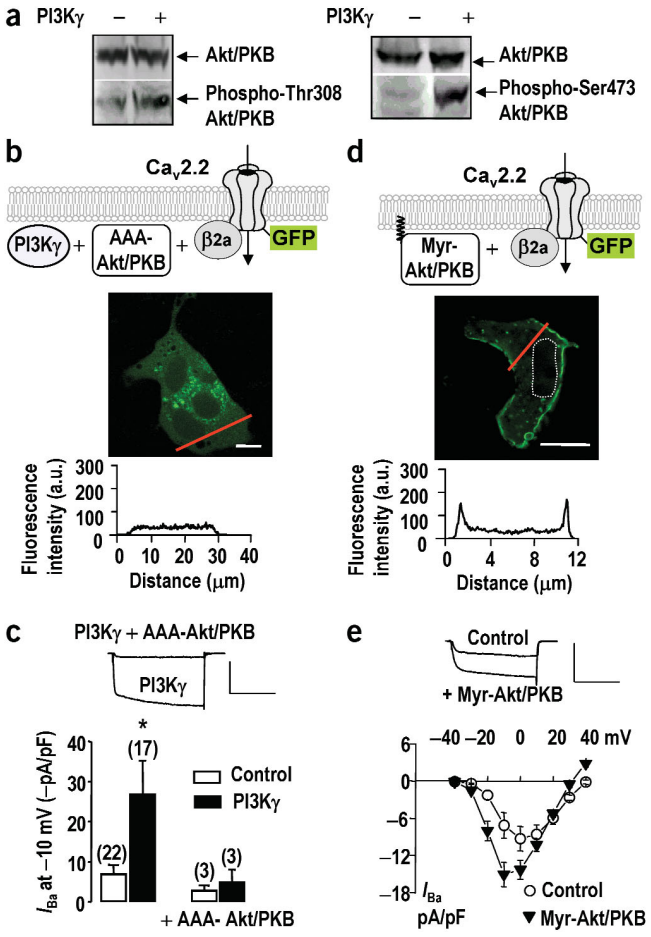

Figure 4 Role of Akt/PKB in the PI3Kγ-induced enhancement of Ca_v expression at the membrane. (**a**) PI3Kγ-induced phosphorylation of endogenous Akt/PKB was measured using phospho-Thr308 (left) or phospho-Ser473 (right) Akt/PKB antibody. Whereas Akt/PKB (arrow, upper row) was immunodetected in both untransfected (lane 1) and PI3Kγ-transfected cells (lane 2), phosphorylated Akt/PKB (arrow, lower row) was detected only in PI3Kγ-transfected cells (lane 2). (**b**) Effect of AAA-Akt/PKB mutant on GFP-$Ca_v2.2\alpha1/\beta_{2a}$ subcellular localization in PI3Kγ-transfected cells. Scale bars, 10 μm. (**c**) Top, sample traces of $Ca_v2.2\alpha1/\beta_{2a}$ I_{Ba} recorded in PI3Kγ-transfected cells without or with AAA-Akt/PKB. Below, effect of AAA-Akt/PKB mutant on $Ca_v2.2\alpha1/\beta_{2a}$ I_{Ba} in control or PI3Kγ-transfected cells. The number of experiments is given in parentheses. $^*P < 0.05$ as compared to control. (**d**,**e**) Effect of myr-Akt/PKB on GFP-$Ca_v2.2\alpha1/\beta_{2a}$ subcellular localization (**d**) and on $Ca_v2.2\alpha1/\beta_{2a}$ channel currents (**e**). Top in **e**, example traces of $Ca_v2.2\alpha1/\beta_{2a}$ I_{Ba} recorded in control and myr-Akt/PKB-transfected cells. Vertical and horizontal scales were 20 pA/pF and 100 ms, respectively. Below, mean *I-V* relationship of $Ca_v2.2\alpha1/\beta_{2a}$ channels in control or myr-Akt/PKB-transfected cells. Results are expressed as mean ± s.e.m. of 8–18 cells.

vented the PI3Kγ-induced increase of the mean $Ca_v2.2\alpha1/\beta_{2a}$ I_{Ba} (**Fig. 4c**), indicating that AAA-Akt/PKB may counteract the effect of PI3Kγ on Ca_v channel trafficking.

Second, because translocation of Akt/PKB to the membrane is sufficient to promote its partial activation[6], we coexpressed a myristoylated Akt/PKB (myr-Akt/PKB) with $Ca_v2.2$ channels. Myr-Akt/PKB produced a significant increase of both GFP-$Ca_v2.2/\beta2a$ channel accumulation at the membrane (**Fig. 4d**) and $Ca_v2.2/\beta_{2a}$ I_{Ba} (**Fig. 4e**). The maximum conductance was increased to 0.44 ± 0.05 nS/pF ($n = 18$; $P < 0.05$). There was also a small hyperpolarization of the *I-V* relationship (by –7.7 ± 0.8 mV; $n = 18$; $P < 0.0001$) (**Fig. 4e**). Both the relative increase in localization to the plasma membrane as compared to cytosol (73 ± 4%; $n = 15$ cells) and the increase in currents obtained with myr-Akt/PKB were smaller than those measured with PI3Kγ, indicating that maximal activation of Akt/PKB also requires production of PIP_3.

To determine whether these effects were additive, we transfected both PI3Kγ and myr-Akt/PKB with the Ca_v channels. Both the localization of GFP-$Ca_v2.2/\beta_{2a}$ channels at the plasma membrane and the $Ca_v2.2/\beta_{2a}$ I_{Ba} were increased, although to the same extent as with PI3Kγ expression alone (**Supplementary Fig. 2** online), indicating that PI3Kγ and Akt/PKB are part of the same transduction pathway. The total amount of $Ca_v2.2\alpha1$ expressed was similar in both populations of control and PI3Kγ-CAAX/myr-PKB-transfected cells (**Supplementary Fig. 3** online), indicating that the effect of PI3Kγ and Akt/PKB on the plasma membrane localization of Ca_v channels is not primarily due to increased $Ca_v2.2\alpha1$ synthesis or decreased catabolism but rather to the enhanced targeting of the Ca_v channels to the plasma membrane.

Together, these data indicate that Akt/PKB mediates the effect of PI3Kγ/PIP_3 on the trafficking of functional Ca_v channels to the plasma membrane.

Role of serine 574 of $Ca_v\beta_{2a}$

We identified a unique putative consensus site (RxRxxS) for phosphorylation by Akt/PKB[25] in the C-terminal domain of $Ca_v\beta_2$, which was absent from β_{1b}, β_3 and β_4 subunits (**Supplementary Fig. 4** online). We constructed two mutants of $Ca_v\beta_{2a}$. In the first, $Ca_v\beta_{2a}$S574A, Ser574 was replaced by alanine to prevent phosphorylation. In the second, $Ca_v\beta_{2a}$S574E, it was replaced by glutamate to mimic phosphorylation.

Expression of both PI3Kγ and myr-Akt/PKB failed to increase the targeting of GFP-$Ca_v2.2/\beta_{2a}$S574A to the plasma membrane (**Fig. 5a–c**). The $Ca_v2.2/\beta_{2a}$S574A channels were functional, though insensitive to PI3Kγ (**Fig. 5b**) and to myr-Akt/PKB (**Fig. 5d**).

The S574A mutation also prevented the increase in $Ca_v\beta_{2a}$ phosphorylation induced by PI3Kγ coexpression (**Fig. 5e–g**) (see **Supplementary Methods** online). One further argument for the involvement of Akt/PKB in this modulation is that Akt/PKB coimmunoprecipitated with the $Ca_v\beta_{2a}$ subunits (**Fig. 5h**), indicating that this kinase may act directly on $Ca_v\beta_{2a}$.

Finally, expression of GFP-$Ca_v2.2/\beta_{2a}$S574E, in the absence of PI3Kγ, was sufficient to increase the targeting of GFP-$Ca_v2.2$ channels to the plasma membrane (80 ± 2% increase as compared to cytosol; $n = 25$ cells). The distribution patterns, either continuous or in punctate clusters, were similar to those showed by GFP-$Ca_v2.2/\beta_{2a}$ coexpressed with PI3Kγ (**Fig. 6a**). The strong plasma membrane staining was visible on all focal planes of acquisition (**Supplementary Video 2** online). The S574E mutation also increased $Ca_v2.2/\beta_2$ I_{Ba} by an extent similar to PI3Kγ expression (**Fig. 6b**). Coexpression of the dominant-negative mutant AAA-Akt/PKB with GFP-$Ca_v2.2/\beta_{2a}$S574E did not prevent the recruitment of the channels to the plasma membrane (data not shown), indicating that the S574E mutation may relieve the requirement for Akt/PKB. Moreover, coexpression of both PI3Kγ-CAAX and myr-Akt/PKB together with GFP-$Ca_v2.2/\beta_{2a}$S574E did not further increase the trafficking of the channels to the membrane (data not shown), confirming that the S574E mutation bypasses the PI3K-activated pathway.

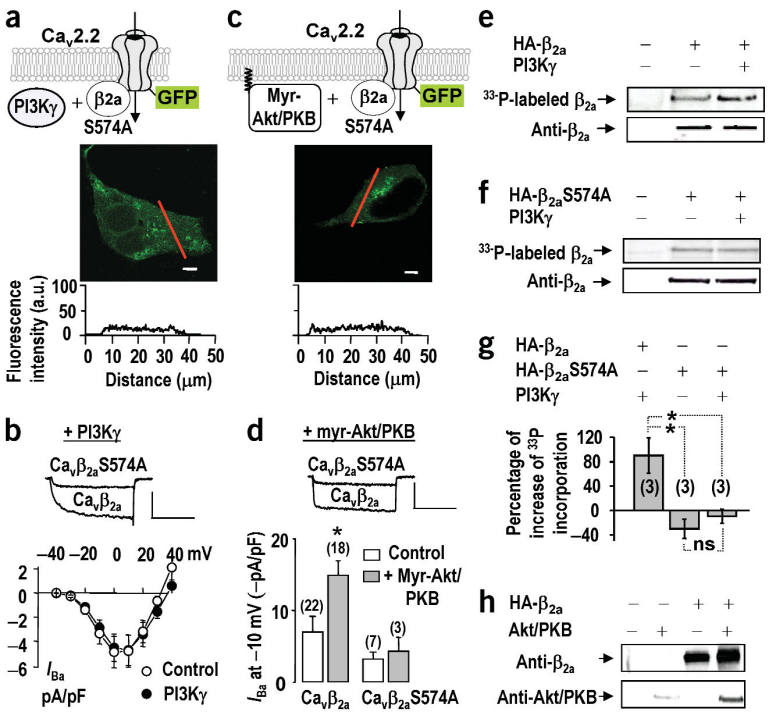

Figure 5 Effect of S574A mutation on the PI3Kγ and myr-Akt/PKB-induced regulation of $Ca_v2.2$ channels. (**a**) Subcellular localization of GFP-$Ca_v2.2\alpha1/\beta_{2a}$S574A channels in PI3Kγ-transfected cells. (**b**) Top, sample current traces of $Ca_v2.2\alpha1$ channels cotransfected with PI3Kγ and either wild-type $Ca_v\beta_{2a}$ or $Ca_v\beta_{2a}$S574A mutant. Below, mean *I-V* relationship of GFP-$Ca_v2.2\alpha1/\beta_{2a}$S574A channels in control and PI3Kγ-transfected cells. (**c**) Subcellular localization of GFP-$Ca_v2.2\alpha1/\beta_{2a}$S574A channels in myr-Akt/PKB-transfected cells. (**d**) Top, sample current traces of $Ca_v2.2\alpha1$ channels cotransfected with myr-Akt/PKB and either wild-type $Ca_v\beta_{2a}$ or $Ca_v\beta_{2a}$S574A mutant. Vertical and horizontal scales are 10 pA/pF and 100 ms, respectively. Below, I_{Ba} for channels formed with $Ca_v2.2\alpha1$ and either $Ca_v\beta_{2a}$ or β_{2a}(S574A) in control (open bars) or myr-Akt/PKB-transfected cells (gray bars). The number of experiments is given in parentheses. $^*P < 0.05$ as compared to control. (**e**,**f**) PI3Kγ-induced phosphorylation of $Ca_v\beta_{2a}$. Cells were transfected with $Ca_v\beta_{2a}$ (**e**) or β_{2a}S574A (**f**) either with or without PI3Kγ as indicated. Upper row, amount of ^{33}P incorporated into $Ca_v\beta_{2a}$; lower row, amount of $Ca_v\beta_{2a}$ protein as assessed by western blotting with anti-$Ca_v\beta_{2a}$ antibodies. (**g**) Comparison of ^{33}P incorporation into $Ca_v\beta_{2a}$ coexpressed with PI3Kγ and $Ca_v\beta_{2a}$S574A alone or coexpressed with PI3Kγ. $^*P < 0.05$; ns, nonsignificant. (**h**) Coimmunoprecipitation of $Ca_v\beta_{2a}$ and Akt/PKB. (For details of **Fig. 5e–h**, see **Supplementary Methods** online.)

These results indicate that phosphorylation of $Ca_v\beta_2$ subunits is necessary and sufficient to support the PI3K- and Akt/PKB-induced enhancement of functional Ca_v channel expression at the plasma membrane.

Effect of PI3Kα on Ca_v membrane expression

The scavenging effect of GFP-PH_{Grp1} indicates that PIP_3 mediates the effect of PI3Kγ on Ca_v channels. We therefore examined whether another PIP_3-producing PI3K, PI3Kα, could also regulate Ca_v channel trafficking. The overexpression of PI3Kα (p85-p110α), like that of PI3Kγ, was sufficient to recruit the GFP-PH_{Grp1} domain to the plasma membrane (**Fig. 7a**), which is indicative of PIP_3 production. As in the experiments performed with PI3Kγ, the expression at the plasma membrane of $Ca_v2.2/\beta_{2a}$ channels was also increased in cells cotransfected with PI3Kα (**Fig. 7b**). The relative increase in plasma membrane as compared to cytosolic localization in PI3Kα-transfected cells was 85 ± 2% (n = 15 cells). No effect of PI3Kα was detected on Ca_v channel trafficking when $Ca_v2.2$ was coexpressed with $Ca_v\beta_{2a}$S574A (**Fig. 7c**) or $Ca_v\beta_{1b}$ (**Fig. 7d**) instead of $Ca_v\beta_{2a}$. These results indicate that a sustained production of PIP_3, independently of the PI3K isoform or activation pathway, increases Ca_v channel trafficking to the plasma membrane.

Effect in neurons

To investigate whether activation of the PI3K/Akt/PKB pathway could induce the translocation of Ca_v channels in neurons, we transiently transfected rat dorsal root ganglion (DRG) neurons with GFP-$Ca_v2.2/\beta_{2a}$ channels. Rat DRG neurons have previously been shown by quantitative PCR to express $Ca_v\beta_2$ subunits[26], and protein expression of $Ca_v\beta_2$ in these neurons was confirmed by immunoblotting (data not shown). DRG neurons were deprived of serum for 24 h before experiments. After 5 min of exposure to IGF-1, PH_{GRP1}-GFP was translocated to the plasma membrane (**Fig. 8a**) and Akt/PKB was phosphorylated (**Fig. 8b**), indicative of PI3K-induced production of PIP_3 and activation of Akt/PKB, respectively. We compared in parallel two sets of neurons, either controls (**Fig. 8c**) or those preincubated at 37 °C for 30 min with IGF-1 (**Fig. 8d**). IGF-1 induced a stronger expression of GFP-Ca_v/β_{2a} channels at the plasma membrane in 55 ± 9% (n = 36; four independent experiments) of the preincubated neurons. We measured the fluorescence intensity over a 4-μm distance

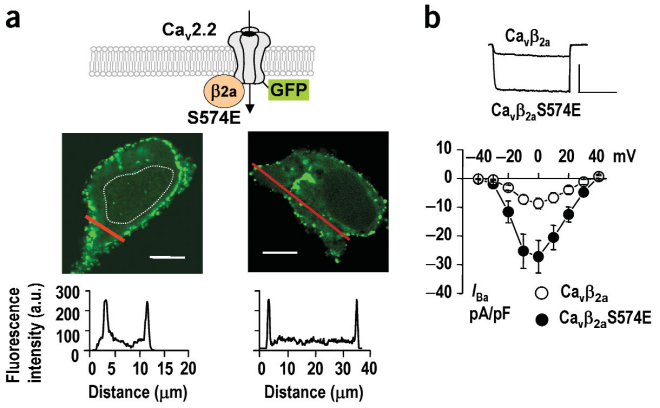

Figure 6 Effect of $Ca_v\beta_{2a}$S574E mutant on $Ca_v2.2$ channel expression at the membrane. (**a**) Examples of subcellular localization of GFP-$Ca_v2.2\alpha1/\beta_{2a}$S574E channels. Scale bars, 10 μm. (**b**) Top, sample current traces of $Ca_v2.2\alpha1$ channels cotransfected with wild-type $Ca_v\beta_{2a}$ and $Ca_v\beta_{2a}$S574E mutant. Vertical and horizontal scales were 20 pA/pF and 100 ms, respectively. Below, mean *I-V* relationship of GFP-$Ca_v2.2\alpha1/\beta_{2a}$ and GFP-$Ca_v2.2\alpha1/\beta_{2a}$S574E channels in the absence of PI3Kγ.

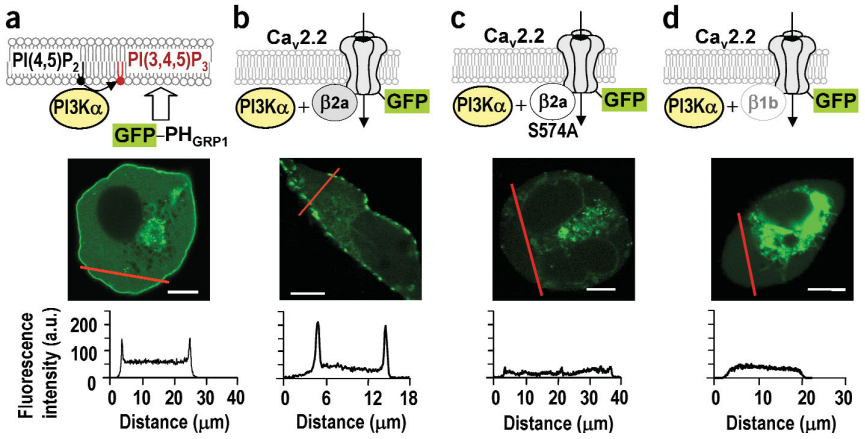

Figure 7 Effect of PI3Kα on PH_{Grp1}-GFP and Ca_v channel membrane localization. (**a**) Subcellular localization, in PI3Kα-transfected cells, of PH_{Grp1}-GFP. (**b**) GFP-$Ca_v2.2\alpha1/\beta_{2a}$. (**c**) GFP-$Ca_v2.2\alpha1/\beta_{2a}$S574A. (**d**) GFP-$Ca_v2.2\alpha1/\beta_{1b}$. Scale bars, 10 μm.

covering the membrane and the immediate cytosol in 18 IGF-1-responsive neurons and 18 parallel controls. The cells preincubated with IGF-1 showed a 28 ± 4% increase in fluorescence at the plasma membrane as compared to the cytosol, whereas the control cells showed an increase of only 4 ± 2% ($P < 0.00005$). These percentages correspond to an approximately sixfold greater effect in IGF-1-treated neurons as compared to control neurons, which indicates clearly that the IGF-1 pretreatment promoted the expression of GFP-Ca_v channels at the plasma membrane.

DISCUSSION

Our experiments show that an increase of PIP_3 stimulates trafficking of Ca_v channels to the plasma membrane. Although it is possible that $PI(4,5)P_2$ depletion may also partially contribute to the PI3Kγ-induced increase of Ca_v currents[27], we show here that the PI3Kγ-induced increase in Ca_v current density was blocked by the PIP_3-scavenging PH_{GRP1}-GFP domain, indicating that it is the production of PIP_3 rather than a decrease in PIP_2 that mediates the PI3Kγ-induced effect. Furthermore, an increase in 3-phosphoinositides is required to activate Akt/PKB, which mediates the PI3Kγ-induced increase of Ca_v channel expression at the membrane. The Akt/PKB-PH domain binds either $PI(3,4)P_2$ or PIP_3 *in vitro*[15] and $PI(3,4)P_2$ can be produced by dephosphorylation of PIP_3 (ref. 5). Therefore, it is possible that not only PIP_3 but also $PI(3,4)P_2$ contributes to the promotion of trafficking of Ca_v channels.

PI3K promotes the membrane insertion of nonselective cation channels[21] and calcium-dependent potassium channels[28], but the mechanisms involved are still unknown. A role for PI3K in the reorganization of the actin cytoskeleton, which contributes to the transport of proteins inside the cell, has also been described[29]. Several recent studies have also reported a role for Akt/PKB in trafficking. Akt/PKB mediates the translocation of glucose transporters induced by insulin in myoblasts through an unknown mechanism[23]. Notably, association with the annexin p11 (ref. 30) or 14-3-3 proteins[31,32] has been shown to promote trafficking of potassium channels to the membrane and the 14-3-3 proteins have been reported to bind to Akt/PKB phosphorylated sites[32]. One might thus speculate that phosphorylation of $Ca_v\beta_{2a}$ by Akt/PKB could induce the association of the Ca_v channel complexes with trafficking proteins to promote their translocation to the plasma membrane. This does not, however, exclude the involvement of other kinases or of additional phosphorylation targets for Akt/PKB.

$Ca_v\beta$ subunits have been reported to antagonize an unidentified endoplasmic reticulum retention signal located in the I-II loop of $Ca_v\alpha1$ subunits[33]. Here we show that one particular $Ca_v\beta$, $Ca_v\beta_2$, also promotes the trafficking of Ca_v channels to the plasma membrane by supporting the regulation induced by PI3K. $Ca_v\beta_{2a}$ has been reported to be a very efficient chaperone protein for $Ca_v2.1$ channel expression at the plasma membrane and this effect was attributed to the palmitoylation specific to $Ca_v\beta_{2a}$[17]. This was confirmed by our experiments

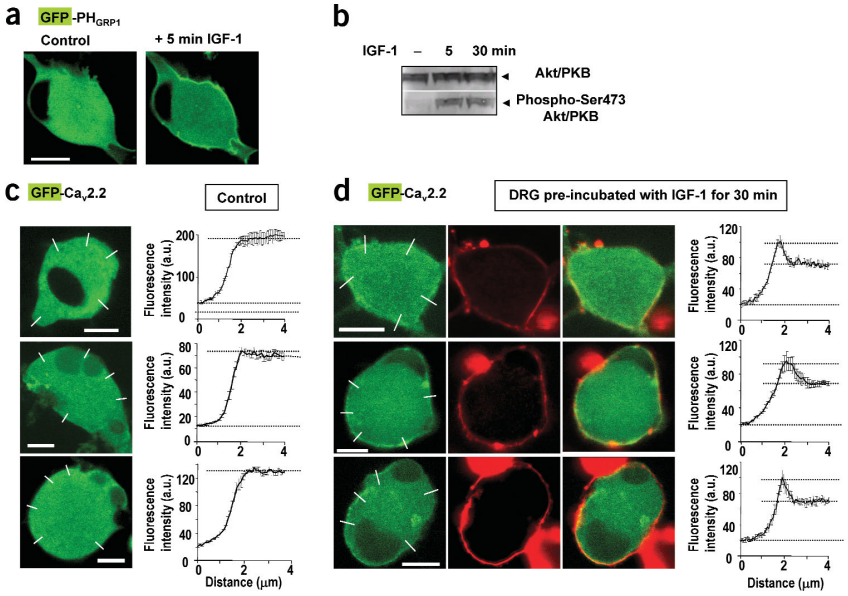

Figure 8 Effect of acute stimulation of PI3K on Ca_v channel localization in DRG neurons. (**a**) Distribution of PH_{Grp1}-GFP before (left) and after 5 min incubation with 200 ng/ml IGF-1 (right). (**b**) Total Akt/PKB (upper row) and Akt/PKB phosphorylated on Ser473 (lower row) as measured by immunoblotting in control neurons and those preincubated with IGF-1 for 5 or 30 min. (**c**) Subcellular localization of GFP-$Ca_v2.2\alpha1/\beta_{2a}$ in three control neurons and averaged intensity profile corresponding to the five segments of the cell indicated by the white lines on the micrographs. (**d**) Left, effect of IGF-1 on subcellular localization of GFP-$Ca_v2.2\alpha1/\beta_{2a}$ in three different representative neurons preincubated with IGF-1 for 30 min. Middle, plasma membrane staining with the membrane marker FM4-64. Right, overlay of the GFP-$Ca_v2.2\alpha1/\beta_{2a}$ and FM4-64 fluorescence images. The averaged intensity profiles corresponding to the five lines on each micrograph are shown on the far right.

showing that current density with $Ca_v\beta_{2a}$ was higher than with the three other $Ca_v\beta$ subunits (**Fig. 2b–d**) or the non-palmitoylatable mutant of $Ca_v\beta_{2a}$ (**Fig. 2e**). However, we showed that the palmitoylation of $Ca_v\beta_{2a}$ is not involved in the PI3K-induced regulation. The PI3K-induced increase of Ca_v channel density requires the phosphorylation of $Ca_v\beta_{2a}$ on Ser574 in an Akt/PKB consensus site identified only in $Ca_v\beta2$, in its C terminus, which is common to all splice variants. This indicates that PI3K-induced regulation of Ca_v channels may be determined by the cell type and the subcellular distribution of $Ca_v\beta_2$ subunits and provides a key argument in our understanding of the physiological relevance of the multiplicity of $Ca_v\beta$ isoforms. Indeed, $Ca_v\beta_2$ has been shown to associate with L-, N- and P/Q type Ca_v channels[34,35], although to a smaller extent than $Ca_v\beta_{1b}$ and $Ca_v\beta_4$ subunits when measured from whole brain tissue, indicating that the subcellular localization of the Ca_v channels associated with $Ca_v\beta_2$ may be a determining factor for PI3K-induced regulation of neuronal native Ca_v channels.

Ca^{2+} entry activates Akt/PKB in a PI3K-independent manner in neurons, and this regulation protects cells from apoptosis[36]. The Akt/PKB-induced translocation of Ca_v channels that we demonstrate here may thus be involved in a positive feedback to promote cell survival. Indeed, in cerebellar granule neurons, Akt/PKB-induced potentiation of L-type channels has been shown to increase neuronal survival[37]. Our data indicate that PI3K may also mediate changes in excitability by increasing the insertion or prolonging the surface expression of Ca_v channels containing $Ca_v\beta_2$ subunits. The PI3K- and Akt/PKB-induced change in excitability might be of particular importance in pathology such as epilepsy, where $Ca_v\beta_2$ subunits have been shown to be upregulated in hippocampal neurons[38].

METHODS

cDNAs. Rat brain $Ca_V1.2$ (M67515), rabbit $Ca_v2.2\alpha1$ (D14157), N-terminal GFP-tagged rabbit $Ca_V2.2$[22], rat $Ca_V\beta_{1b}$ (X61394), β_{2a} (M80545), β_{2a}(C3,4S)[18], β_3 (M88751), β_4 (L02315), $\alpha2\delta$-1 (M86621) and mut-3b GFP (M62653) cDNAs were subcloned into pMT_2 for expression in COS-7 cells. For expression in neurons, N-terminal GFP-tagged rabbit $Ca_V2.2$ and $Ca_v\beta_{2a}$ were subcloned into pRK5. Mutation of Ser574 to alanine in $Ca_V\beta_{2a}$S574A and of Ser574 to glutamate in $Ca_V\beta_{2a}$S574E was done using the Quikchange site-directed mutagenesis kit (Stratagene). For the biochemistry experiments, the $Ca_V\beta_{2a}$ (C3,4S) 5′ untranslated region was removed and a hemagglutinin (HA) epitope tag was fused to the N-terminus. PI3Kγ was composed of p101 (Y10742) in $pcDNA_3$ and p110γ (X83368) in pMT_2. The membrane-targeted p110γ-CAAX (in $pcDNA_3$) was previously described[39]. PI3Kα was composed of p85α (M61745) and p110α (M93252) both in pSG5. The PH_{Grp1}-GFP[15] was a gift from A. Gray and C.P. Downes (Department of Biochemistry, Univ. Dundee). Mouse Akt/PKB and myr-Akt/PKB, in pUSE-amp, were purchased from Upstate Biotechnology. AAA-Akt/PKB[24] mutant in pcMV5 was provided by D. Alessi (MRC Protein Phosphorylation Unit, Univ. Dundee).

Transfection. Monkey COS-7 cells were cultured as previously described[15]. Transfections were performed either with Geneporter transfection reagent (Gene Therapy Systems; DNA/Geneporter ratio 6μg/30 μl) or Fugene6 (Roche Diagnostics Limited; DNA/Fugene6 ratio 3 μg/6 μl). The $Ca_v\alpha1$, β, p101, p110γ, PKB isoforms or mutants were cotransfected with mut3-GFP in a 3:1:2:2:2:0.2 ratio by DNA weight. The $\alpha2\delta$-1 cDNA was omitted to limit the number of cDNA constructs cotransfected into the cells. In the absence of p101 and p110γ, the corresponding blank vectors were substituted. Akt/PKB mutants were substituted by pMT_2 and PH_{Grp1}-GFP by mut3-GFP. Experiments were performed 3–4 d after transfection. Dorsal root ganglion neurons isolated from adult Sprague-Dawley rats were dissociated and transfected with the Amaxa nucleofector I (Amaxa Biosystems) following the manufacturer's instructions. Neurons were plated on glass-bottomed dishes (MatTek) coated with polyornithine (0.5 mg/ml) and cultured for 48 h before the experiments. We examined all the cells successfully transfected with the GFP-tagged channels with or without treatment with IGF-1. All materials were from Sigma unless otherwise stated.

Electrophysiology. Cells were re-plated using a nonenzymatic cell dissociation solution (Sigma) and maintained at 27 °C for between 2 and 8 h. Recordings were made from fluorescent COS-7 cells expressing mut3-GFP. Borosilicate glass electrodes (2–5 MΩ) were filled with (mM): cesium aspartate, 140; EGTA, 10; $MgCl_2$, 2; magnesium ATP, 5; and HEPES, 10; pH 7.4. The external solution contained (mM): TEA-Br, 160; KCl, 3; $NaHCO_3$, 1; $MgCl_2$, 1; HEPES, 10; glucose, 4; and $BaCl_2$, 1 or 10 when stated; pH 7.4. Whole-cell currents were elicited every 15 s from a holding potential of 80 mV and recorded, at room temperature, using an Axopatch200A amplifier (Axon Instruments). Data were filtered at 1 kHz, digitized at 5 kHz and analyzed using pCLAMP 6 and Origin 5.0 software. Current records are shown after leak and capacitance current subtraction (P/4 protocol). The maximum conductances were calculated by fitting *I-V* relationships with a modified Boltzmann equation. Statistical analysis was performed using unpaired Student's *t*-test.

Confocal imaging. Confocal images were acquired with a Zeiss LSM-510 confocal laser scanning microscope, using a ×40 (1.3 NA) or ×63 (1.4 NA) oil-immersion objective. Optical slices were 1.5 μm thick . The nucleus and the plasma membrane were stained with 1 μg/ml Hoechst 33342 or 1 μM FM4-64 (Molecular Probes), respectively. Images were acquired using an argon laser (excitation, 488 nm; emission, BP505–530 nm emission filter) for GFP-$Ca_v2.2\alpha1$, a UV laser for excitation and a BP385–470 nm emission filter for Hoechst 33342, and a He-Ne laser (excitation, 543 nm; emission filter, LP650 nm) for FM4-64. The outline of the nuclei is indicated by a dotted white line in relevant figures, to emphasize that it is not responsible for membrane localization of GFP-tagged $Ca_v2.2$. Data illustrated are representative of 20–25 cells from at least three independent experiments. Line intensity profiles generated with Metamorph (Universal Imaging) are indicated in red and displayed below each confocal image. To measure the relative increase in plasma membrane localization, we measured the fluorescence intensity over a distance covering the membrane and the immediate cytosol. Three to five line profiles, distributed as regularly as possible, avoiding the nucleus, were performed to obtain an average profile of fluorescence intensity representative of the staining at the perimeter of each cell. The difference between the peak and the plateau of fluorescence was divided by the maximum fluorescence measured along the linescan to give the percentage increase in fluorescence at the membrane. Scale bars are 10 μm.

Note: Supplementary information is available on the Nature Neuroscience website.

ACKNOWLEDGMENTS

We thank K. Chaggar, W.S. Pratt, J. Wratten and M. Nieto-Rostro for technical assistance and K. Page, A. Babich and N.S. Berrow for discussions. This work was supported by the Wellcome Trust and Medical Research Council (UK).

COMPETING INTERESTS STATEMENT

The authors declare that they have no competing financial interests.

Received 3 March; accepted 7 July 2004
Published online at http://www.nature.com/natureneuroscience/

1. Catterall, W.A. Structure and regulation of voltage-gated Ca^{2+} channels. *Annu. Rev. Cell Dev. Biol.* **16**, 521–555 (2000).
2. Dolphin, A.C. Assembly and targeting of voltage-dependent calcium channels. in *Receptor and Ion Channel Trafficking* (eds. Moss, S.J. & Henley, J.) 58–86 (Oxford Univ. Press, Oxford, 2002).
3. Viard, P.*et al.* Gβγ dimers stimulate vascular L-type Ca^{2+} channels via phosphoinositide 3-kinase. *FASEB J.* **13**, 685–694 (1999).
4. Blair, L.A. & Marshall, J. IGF-1 modulates N- and L-type calcium channels in a PI 3 kinase-dependent manner. *Neuron* **19**, 421–429 (1997).
5. Rameh. L.E. and Cantley, L.C. The role of phosphoinositide 3-kinase lipid products in cell function. *J. Biol. Chem.* **274**, 8347–8350 (1999).
6. Andjelkovic, M. *et al.* Role of translocation in the activation and function of protein kinase B. *J. Biol. Chem.* **272**, 31515–31524 (1997).
7. Vanhaesebroeck, B. *et al.* Synthesis and function of 3-phosphorylated inositol lipids. *Annu. Rev. Biochem.* **70**, 535–602 (2001).
8. Rodriguez-Viciana, P. *et al.* Phosphatidylinositol-3-OH kinase as a direct target of Ras. *Nature* **370**, 527–532 (1994).

9. Pacold, M.E. *et al.* Crystal structure and functional analysis of Ras binding to its effector phosphoinositide 3-kinase γ. *Cell* **103**, 931–943 (2000).
10. Kurosu, H. *et al.* Heterodimeric phosphoinositide 3-kinase consisting of p85 and p110β is synergistically activated by the βγ subunits of G proteins and phosphotyrosyl peptide. *J. Biol. Chem.* **272**, 24252–24256 (1997).
11. Murga, C., Laguinge, L., Wetzker, R., Cuadrado, A. & Gutkind, J.S. Activation of Akt/protein kinase B by G protein–coupled receptors. A role for α and βγ subunits of heterotrimeric G proteins acting through phosphatidylinositol-3-OH kinase gamma. *J. Biol. Chem.* **273**, 19080–19085 (1998).
12. Maier, U., Babich, A. & Nürnberg, B. Roles of non-catalytic subunits in Gβγ-induced activation of class I phosphoinositide 3-kinase β and γ. *J. Biol. Chem.* **274**, 29311–29317 (1999).
13. Stephens, G.J., Brice, N.L., Berrow, N.S. & Dolphin, A.C. Facilitation of rabbit α1B calcium channels: involvement of endogenous Gβγ subunits. *J. Physiol. (Lond.)* **509**, 15–27 (1998).
14. Lopez-Ilasaca, M.L., Crespo, P., Pellici, P.G., Gutkind, J.S. & Wetzker, R. Linkage of G protein–coupled receptors to the MAPK signaling pathway through PI 3-kinase γ. *Science* **275**, 394–397 (1997).
15. Gray, A., Van Der Kaay, J. & Downes, C.P. The pleckstrin homology domains of protein kinase B and GRP1 (general receptor for phosphoinositides-1) are sensitive and selective probes for the cellular detection of phosphatidylinositol 3,4-bisphosphate and/or phosphatidylinositol 3,4,5-trisphosphate *in vivo*. *Biochem. J.* **344**, 29–36 (1999).
16. Bondeva, T. *et al.* Bifurcation of lipid and protein kinase signals of PI3Kγ to the protein kinases PKB and MAPK. *Science* **282**, 293–296 (1998).
17. Chien, A.J., Carr, K.M., Shirokov, R.E., Rios, E. & Hosey, M.M. Identification of palmitoylation sites within the L-type calcium channel β2a subunit and effects on channel function. *J. Biol. Chem.* **271**, 26465–26468 (1996).
18. Stephens, G.J., Page, K.M., Bogdanov, Y. & Dolphin, A.C. The α1B Ca^{2+} channel amino terminus contributes determinants for β subunit-mediated voltage-dependent inactivation properties. *J. Physiol. (Lond.)* **525**, 377–390 (2000).
19. Brice, N.L. *et al.* Importance of the different β-subunits in the membrane expression of the α1A and α2 calcium channel subunits: studies using a depolarisation-sensitive α1A antibody. *Eur. J. Neurosci.* **9**, 749–759 (1997).
20. Chien, A.J. *et al.* Roles of a membrane-localized β subunit in the formation and targeting of functional L-type Ca2+ channels. *J. Biol. Chem.* **270**, 30036–30044 (1995).
21. Kanzaki, M. *et al.* Translocation of a calcium-permeable cation channel induced by insulin-like growth factor-1. *Nat. Cell Biol.* **1**, 165–170 (1999).
22. Raghib, A. *et al.* Dominant-negative synthesis suppression of voltage-gated calcium channel Cav2.2 induced by truncated constructs. *J. Neurosci.* **21**, 8495–8504 (2001).
23. Wang, Q. *et al.* Protein kinase B/Akt participates in GLUT4 translocation by insulin in L6 myoblasts. *Mol. Cell. Biol.* **19**, 4008–4018 (1999).
24. Bertrand, L. *et al.* Heart 6-phosphofructo-2-kinase activation by insulin results from Ser-466 and Ser-483 phosphorylation and requires 3-phosphoinositide-dependent kinase-1, but not protein kinase B. *J. Biol. Chem.* **274**, 30927–30933 (1999).
25. Obata, T. *et al.* Peptide and protein library screening defines optimal substrate motifs for Akt/PKB. *J. Biol. Chem.* **275**, 36108–36115 (2000).
26. Martin, D.J. *et al.* Gabapentin-mediated inhibition of voltage-activated Ca^{2+} channel currents in cultured sensory neurones is dependent on culture conditions and channel subunit expression. *Neuropharmacology* **42**, 353–366 (2002).
27. Wu, L., Bauer, C.S., Zhen, X.G., Xie, C. & Yang, J. Dual regulation of voltage-gated calcium channels by PtdIns(4,5)P_2. *Nature* **419**, 947–952 (2002).
28. Lhuillier, L. & Dryer, S.E. Developmental regulation of neuronal K_{Ca} channels by GFβ1: an essential role for PI3 kinase signaling and membrane insertion. *J. Neurophysiol.* **88**, 954–964 (2002).
29. Insall, R.H. & Weiner, O.D. PIP3, PIP2, and cell movement—Similar messages, different meanings? *Dev. Cell* **1**, 743–747 (2001).
30. Girard, C. *et al.* p11, an annexin II subunit, an auxiliary protein associated with the background K^+ channel, TASK-1. *EMBO J.* **21**, 4439–4448 (2002).
31. Rajan, S. *et al.* Interaction with 14-3-3 proteins promotes functional expression of the potassium channels TASK-1 and TASK-3. *J. Physiol. (Lond.)* **545**, 13–26 (2002).
32. O'Kelly, I., Butler, M.H., Zilberberg, N. & Goldstein, S.A. Forward transport. 14-3-3 binding overcomes retention in endoplasmic reticulum by dibasic signals. *Cell* **111**, 577–588 (2002).
33. Bichet, D. *et al.* The I–II loop of the Ca^{2+} channel α1 subunit contains an endoplasmic reticulum retention signal antagonized by the β subunit. *Neuron* **25**, 177–190 (2000).
34. Pichler, M. *et al.* β subunit heterogeneity in neuronal L-type Ca^{2+} channels. *J. Biol. Chem.* **272**, 13877–13882 (1997).
35. Scott, V.E.S. *et al.* β subunit heterogeneity in N-type Ca^{2+} channels. *J. Biol. Chem.* **271**, 3207–3212 (1996).
36. Yano, S., Tokumitsu, H. & Soderling, T.R. Calcium promotes cell survival through CaM-K Kinase activation of the protein-kinase-B pathway. *Nature* **396**, 584–587 (1998).
37. Blair, L.A. *et al.* Akt-dependent potentiation of L channels by insulin-like growth factor-1 is required for neuronal survival. *J. Neurosci.* **19**, 1940–1951 (1999).
38. Lie, A.A. *et al.* Distribution of voltage-dependent calcium channel β subunits in the hippocampus of patients with temporal lobe epilepsy. *Neuroscience* **93**, 449–456.
39. Brock, C. *et al.* Roles of Gβγ in membrane recruitment and activation of p110γ/p101 phosphoinositide 3-kinase γ. *J. Cell Biol.* **160**, 89–99 (2003).